

Indirect-to-Direct Bandgap Transition of GeSn by Phonon-assisted Tunneling Spectra in Esaki Diodes

Chia-You Liu^{1*}, Po-Yuan Chiu¹, Yen Chuang¹, and Jiun-Yun Li^{1,2**}

¹ Graduate Institute of Electronics Engineering, National Taiwan University, Taipei, Taiwan 10617

² Taiwan Semiconductor Research Institute, Hsinchu, Taiwan 30078

E-mail: *f05943058@ntu.edu.tw; **jiunyun@ntu.edu.tw

Abstract

Phonon-assisted tunneling spectra in GeSn Esaki diodes were demonstrated to determine the direct-to-indirect bandgap transition in GeSn alloys at 4 K. The phonon signals are clearly observed in Ge and strained Ge_{0.92}Sn_{0.08} diodes, while for relaxed Ge_{0.92}Sn_{0.08} devices, there were no phonon signatures. The results suggest that the indirect-to-direct bandgap transition occurs at a lower Sn fraction of < 8% in relaxed GeSn than in strained GeSn (> 8%).

1. Introduction

GeSn alloys attract a lot of attentions for optoelectronic and electronic device applications due to its direct bandgap nature [1] and high carrier mobility [2], respectively. GeSn alloy becomes a direct-bandgap material as its Sn fraction is above 6 ~ 12 %, depending on the strain condition [3]. Most of the prior work on the transition of indirect-to-direct bandgap in GeSn were done by photoluminescence measurements [4]. In this work, the transition was determined by phonon-assisted tunneling spectra in GeSn Esaki diodes. Our results show that the phonon-assisted tunneling processes occurs in Ge and strained Ge_{0.92}Sn_{0.08} tunnel diodes while for relaxed Ge_{0.92}Sn_{0.08} devices, phonons do not participate the tunneling process. This further verifies that the indirect-to-direct bandgap transition occurs at a lower Sn fraction in the relaxed GeSn than in strained GeSn [5].

2. Experiment

Epitaxial structures of Ge and GeSn Esaki diodes are shown in Fig. 1. The epitaxial films were deposited by reduced pressure chemical vapor deposition (RPCVD) at low temperatures to prevent Sn segregation and precipitates. The precursors for GeSn and Ge growth were Ge₂H₆ and SnCl₄ with B₂H₆ and PH₃ as in-situ dopant gases. For all structures, a 100-nm Ge buffer layer was grown on a Si substrate, followed by in-situ H₂ annealing at 800 °C for the strain relaxation. Heavily-doped p- and n-type layers were subsequently grown to enable band-to-band tunneling. For the relaxed GeSn tunnel diode, the active layers were grown on an additional GeSn relaxed buffer of Ge_{0.88}Sn_{0.12}/Ge_{0.92}Sn_{0.08}/Ge_{0.96}Sn_{0.04} superlattices on top of the relaxed Ge layer [6]. The relaxation rate of the Ge_{0.92}Sn_{0.08} active layer was 92% determined by reciprocal space mapping (RSM). The sub-micron devices were fabricated by e-beam lithography and dry etching. The Ti/Au metal contacts were deposited by e-beam evaporation. Negative differential resistance (NDR) was clearly observed for all devices, which

is crucial for the observation of phonon peaks at low temperatures. The highest peak-to-valley ratios achieved in the relaxed GeSn tunnel diode are 15 and 52 at room temperature and 4 K, respectively [7].

3. Result and Discussion

For indirect-bandgap tunnel diodes, the tunneling process involves the participation of phonons to compensate the momentum difference between electrons in the conduction band and holes in the valence band (Fig. 2). The phonon-assisted tunneling can only be observed in I-V curves at low temperatures due to less thermal broadening [8]. Phonon spectra of tunneling diodes were extracted by the second derivatives of I-V curves at small biases [9]. In practice, large noises would shadow the phonon signatures extracted from the second derivatives of I-V curves. Thus, we followed the procedures in [10] by a harmonic detection system for the extraction of phonon signals.

Fig. 3 shows the spectrum of the second derivative of I-V characteristics of a commercial Ge tunnel diode (1N3717) at 4 K to justify the measurement setup and extraction procedures. The positions of phonon signals are consistent with the phonon energies of Ge [9]. Fig. 4 shows the measured I-V curves, measured dI/dV-V curves, and extracted phonon spectra of the Ge and GeSn devices at 4 K. For epitaxial Ge devices, several phonon peaks in the second derivative spectrum were observed. However, the voltages of phonon peaks are slightly larger than the corresponding phonon peaks for a commercial diode (Fig. 3). This could be due to the series resistance effect [11], shifting the phonon peaks to higher voltages. For the strained Ge_{0.92}Sn_{0.08} device (Fig. 4b), the phonon peaks can be clearly observed in the second derivative spectrum, where the series resistance effect is stronger for the peak positions at higher voltages due to the stronger effects of series resistance. As a result, strained Ge_{0.92}Sn_{0.08} remains an indirect-bandgap material, which is consistent with the photoluminescence results [4]. On the other hand, there was no phonon signal extracted for the relaxed Ge_{0.92}Sn_{0.08} device (Fig. 5). This result suggests that relaxed Ge_{0.92}Sn_{0.08} is a direct-bandgap material, which is consistent with the theoretical calculations [5] and experimental results [12].

3. Conclusions

In this work, the tunneling spectra of Ge and GeSn Esaki diodes at 4 K were demonstrated to determine the indirect-to-direct bandgap transition for GeSn alloys. For the Ge and strained Ge_{0.92}Sn_{0.08} diodes, phonon signatures were clearly observed, while for the relaxed Ge_{0.92}Sn_{0.08} devices, there

were no observable phonon signals, which suggests that the indirect-to-direct bandgap transition for relaxed (strained) GeSn occurs at $[\text{Sn}] \leq (\geq) 8\%$.

Acknowledgements

This work was supported by National Applied Research Laboratories through I-Dream projects (grant number: 13108F1200).

References

[1] S. Gupta et al., *J. Appl. Phys.*, **113**, 073707 (2013).
 [2] S. Takeuchi et al., *Sci. Technol.*, **22**, S231 (2007).
 [3] H. S. Mączko et al., *Sci. Reports* **6**, 34082 (2016).
 [4] S. A. Ghetmiri et al., *Appl. Phys. Letts.* **105**, 151109 (2014).
 [5] L. Liu et al., *J. Appl. Phys.*, **117**, 184501 (2015).
 [6] Y. Chuang et al., *Proc. of 1st ISTDM-ICSI joint conference*, p13 (2018).
 [7] C. Y. Liu et al., *Proc. of 1st ISTDM-ICSI joint conference*, p71 (2018).
 [8] J. Lambe et al., *Phys. Rev.* **165**, 821 (1968).
 [9] A. G. Chynoweth et al., *Phys. Rev.* **125**, 877 (1962).
 [10] M. Bao et al., *IEEE Transactions on Electron Devices* **53**, 2564 (2006).
 [11] J. Y. Li et al., *IEEE Transactions on Electron Devices* **60**, 2479 (2013).
 [12] S. Al-Kabi et al., *J. Electron. Mater.* **45**, 6251 (2016).

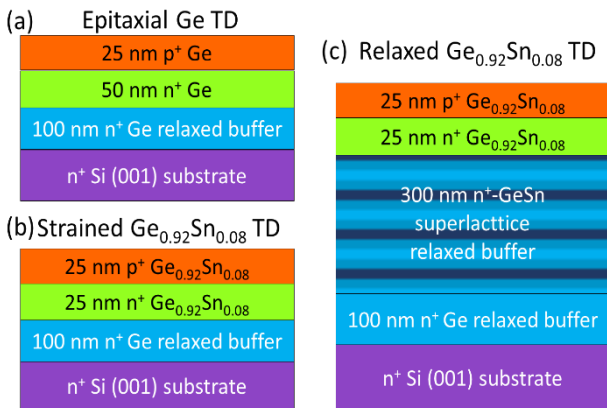


Fig. 1 Epitaxial structures of (a) relaxed Ge and (b) strained $\text{Ge}_{0.92}\text{Sn}_{0.08}$, and (c) relaxed $\text{Ge}_{0.92}\text{Sn}_{0.08}$ Esaki diodes.

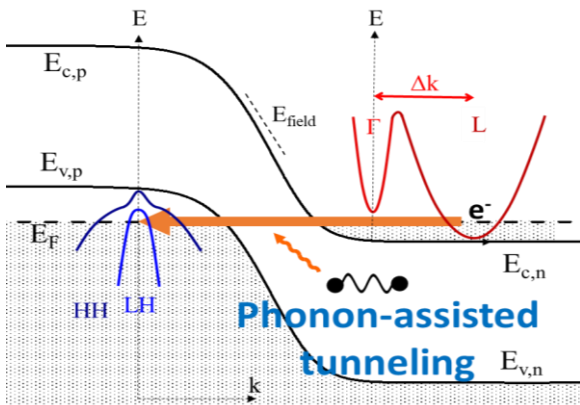


Fig. 2 Energy diagram of phonon-assisted tunneling in indirect-bandgap GeSn.

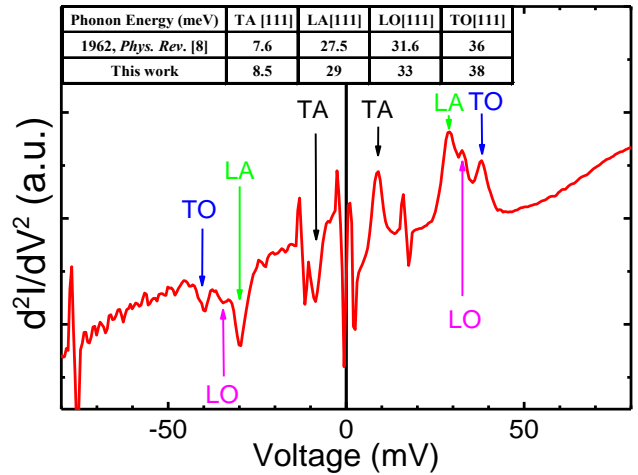


Fig. 3 Phonon-assisted tunneling spectrum of a commercial Ge tunnel diode (1N3717) at 4 K.

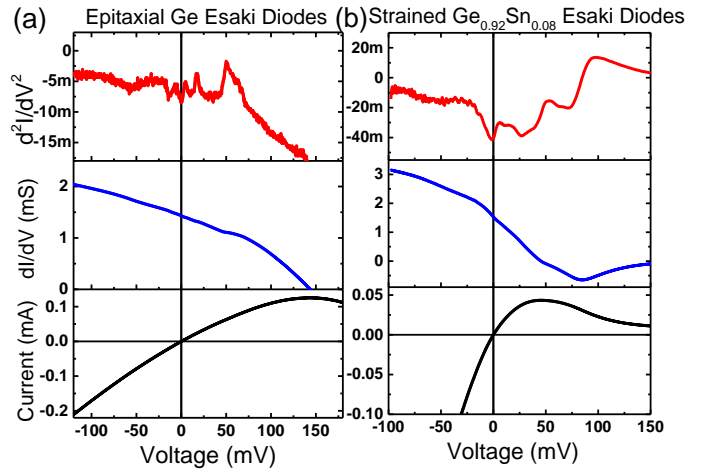


Fig. 4 I-V curves and the associated first and second derivatives of (a) the epitaxial Ge Esaki diode and (b) strained $\text{Ge}_{0.92}\text{Sn}_{0.08}$ Esaki diode at 4 K

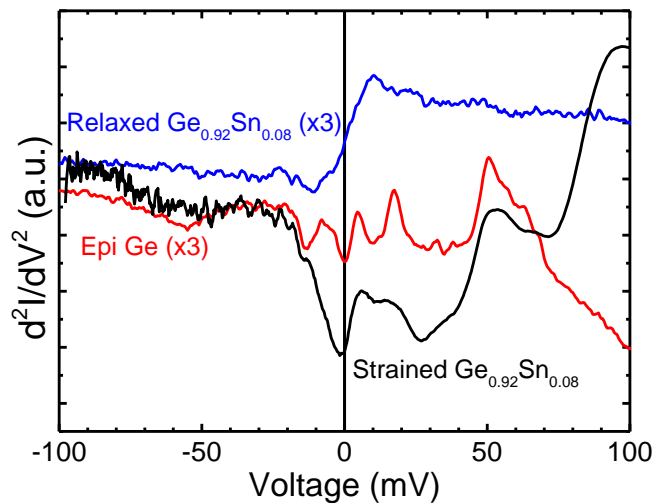


Fig. 5 Tunneling spectra of epitaxial Ge, strained and relaxed $\text{Ge}_{0.92}\text{Sn}_{0.08}$ Esaki diodes.